Published in final edited form as:
J Immunol. 2007 June 15; 178(12): 7598–7606.

Impaired Accumulation of Antigen-Specific CD8 Lymphocytes in Chemokine CCL25-Deficient Intestinal Epithelium and Lamina Propria[1]

Marc-André Wurbel[*,†,‡], **Marie Malissen**[‡], **Delphine Guy-Grand**[§], **Bernard Malissen**[2,‡], and **James J. Campbell**[2,*,†]

* *Department of Dermatology, Brigham and Women's Hospital, Boston, MA 02115*

† *Departments of Dermatology and Pathology, Harvard Medical School, Boston, MA 02115*

‡ *Centre d'Immunologie de Marseille-Luminy, Institut National de la Santé et de la Recherche Médicale (INSERM)-Centre National de la Recherche Scientifique (CNRS)-Université de la Mediterranée, Campus de Luminy, Marseille, France*

§ *Cytokines et Développement Lymphoïde, INSERM Unité 668, Institute Pasteur, Paris, France*

Abstract

CCL25 and CCR9 constitute a chemokine/receptor pair involved in T cell development and in gut-associated immune responses. In this study, we generated CCL25$^{-/-}$ mice to answer questions that could not be addressed with existing CCR9$^{-/-}$ mice. Similar phenotypes were observed for both CCL25$^{-/-}$ and CCR9$^{-/-}$ mice, consistent with the notion that CCL25 and CCR9 interact with each other exclusively. We assessed the requirement for CCL25 in generating CCR9^{high} CD8 intestinal memory-phenotype T cells and the subsequent accumulation of these cells within effector sites. TCR-transgenic naive CD8 T cells were transferred into wild-type or CCL25-deficient hosts. Oral sensitization with Ag allowed these naive donor cells to efficiently differentiate into CCR9^{high} memory-phenotype cells within the mesenteric lymph nodes of wild-type hosts. This differentiation event occurred with equal efficiency in the MLN of CCL25-deficient hosts, demonstrating that CCL25 is not required to induce the CCR9^{high} memory phenotype in vivo. However, we found that CCL25 deficiency severely impaired the Ag-dependent accumulation of donor-derived CD8 T cells within both lamina propria and epithelium of the small intestine. Thus, although CCL25 is not necessary for generating memory-phenotype CD8 T cells with "gut-homing" properties, this chemokine is indispensable for their trafficking to the small intestine.

Interactions between the chemokine CCL25 and its receptor CCR9 are involved in thymic development and in the generation of gut-specific immunological memory (1–3). In the thymus, CCL25-CCR9 interactions appear to play an important role in the migration of early

[1]This work was supported by R01-AI046784 from the National Institutes of Health National Institute of Allergy and Infectious Diseases (to J.J.C.) and a research award from the Crohn's and Colitis Foundation of America (to M.-A.W.). The generation and preliminary characterization of CCL25-deficient mice was performed by M.-A.W. in the laboratory of M.M. and B.M. and was supported by Centre National de la Recherche Scientifique, Institut National de la Santé et de la Recherche Médicale, the European Communities (MUGEN Network of Excellence), Fondation pour la Recherche Médicale (Défis de la Recherche en Allergie), and the RIO/MNG Platform.

2Address correspondence and reprint requests to Dr. James J. Campbell, Department of Dermatology, Brigham and Women's Hospital, 221 Longwood Avenue, Eugene Braunwald Research Center 511, Boston, MA 02115; E-mail address: jcampbell@rics.bwh.harvard.edu or Dr. Bernard Malissen, Centre d'Immunologie de Marseille-Luminy, Parc Scientifique et Technologique de Luminy, Case 906, 13009 Marseille Cedex 09, France; E-mail address: bernardm@ciml.univ-mrs.fr (address requests for CCL25-deficient mice to Dr. B. Malissen).

Disclosures
The authors have no financial conflict of interest.

T cells into the cortex from the subcapsular zone after successful *TCRβ* gene rearrangement (4–7). CCR9 may also play an earlier role in thymic development, either by directly controlling thymic colonization (8–10) or by participating in thymic precursor development within the bone marrow (BM)[3] (6,11,12).

In the gut, CCL25 is strongly expressed by epithelial cells lining the small intestinal villi (2, 13), but is less prominently expressed in the colon (2,14,15). The vast majority of small-intestinal T and B lymphocytes express high levels of CCR9 (3,13). Some T cell subsets are significantly reduced within the intestinal epithelium of CCR9-deficient mice (12,16), suggesting that CCR9 is necessary for steady-state intestinal T cell development and/or gut tropism. Additionally, adoptive transfer assays demonstrate that $CCR9^{+/+}$ lymphocytes are more efficient than $CCR9^{-/-}$ lymphocytes at homing to the small intestine (17).

When studying the effects of CCL25-CCR9 interactions on intestinal immunity, it is difficult to attribute these effects to a direct role in intestinal trafficking rather than an indirect role in thymic development. For example, mature T cells from $CCR9^{-/-}$ mice have developed within an abnormal thymic environment and may therefore lack a normal TCR repertoire. The observed alteration in T cell subset distribution may thus result from a paucity of TCR specificities capable of responding to intestinal Ags, instead of a compromised lymphocyte trafficking mechanism.

Furthermore, new discoveries in the past year have shown that all naive murine CD8 T cells express functional CCR9 (6) and that recent thymic-emigrant CD8 T cells can colonize the gut in a CCR9-dependent manner (18,19). These findings suggest that the role of CCL25-CCR9 interactions in thymic development and intestinal memory are intertwined more extensively than previously believed.

We have generated a mouse strain lacking the *CCL25* gene. After extensive characterization of the new strain, we used these mice to ask whether CCL25-CCR9 interactions are directly required for lymphocyte trafficking to the gut. For this purpose, we developed an adoptive-transfer strategy for studying the role of CCL25 within the main compartments of the small intestine. Mature, Ag-specific naive CD8 T cells, having already completed their development in a thymus with normal CCL25-CCR9 interactions, were transferred into wild-type (WT) or $CCL25^{-/-}$ hosts. This model allowed us to determine whether oral Ag could induce naive peripheral CD8 T cells to differentiate into gut-tropic memory-phenotype CD8 T cells in the absence of CCL25-CCR9 interactions and subsequently traffic to the small intestine in the absence of CCL25-CCR9 interactions.

Materials and Methods

Mice

C57BL/6N (Charles River Laboratories), OT-1-transgenic (Tg) and B6.SJL-*Ptprc*^{a} *Pep3*^{b}/BoyJ (The Jackson Laboratory) and CCL25-deficient (see below) and CCR9-deficient mice (6,16) were bred in the animal facility at the Children's Hospital (Boston, MA), and held under specific pathogen-free (SPF) conditions. All mouse procedures were approved by the Children's Hospital Institutional Animal Care and Use Committee.

[3]Abbreviations used in this paper: BM, bone marrow; WT, wild type; SPF, specific pathogen free; Tg, transgenic; ES, embryonic stem; SPL, spleen; MLN, mesenteric lymph node; PLN, peripheral lymph node; PP, Peyer's patch; LP, lamina propria; LPL, LP lymphocyte; IEL, intraepithelial lymphocyte; CT, cholera toxin; DN, double negative; DP, double positive; SP, single positive; EC, epithelial cell; GALT, gut-associated lymphoid tissue.

Generation of CCL25-deficient mice

A 129/Ola genomic DNA cosmid library was used to screen and isolate a *CCL25* gene. After determining its exon-intron gene organization, part of exon 2 (encoding the ATG initiation codon), and all of exons 3 and 4 (encoding the critical cysteine residues needed for protein folding) were removed and replaced by a LoxP-flanked neomycin resistance gene (*neo*) as depicted (see Fig. 1). The *Sca*I-linearized construct was electroporated into CK35 129 mouse embryonic stem (ES) cells (20). G418 (300 μg/ml) and ganciclovir (2 μM) doubly resistant colonies were screened for homologous recombination by Southern blot using 5′ and 3′ single-copy probes. One diagnostic *Xba*I restriction site was introduced at the 5′ end of the neo cassette, whereas a diagnostic *Bgl*II restriction site was lost in exon 2. Using *Bgl*II-digested DNA, the 5′ probe detects a 9.5-kb recombinant fragment and a 4.3-kb WT fragment (see Fig. 1*B*). Using *Xba*I-digested DNA, the 3′ probe detected a 5.5-kb recombinant fragment and a 8.5-kb WT fragment. Three recombinant ES clones (including clone IIID7 shown in Fig. 1*B*) were found capable of germline transmission. The neomycin-resistance gene was removed by crossing the resulting chimeric males to Deleter mice (21). Germline transmission of the targeted allele was detected by Southern blot and PCR using the primers: 5′-ATAGGTGGCC CCCTTAAACCT-3′ (TK26), 5′-GAATTCTTGTTATGCCCAACC-3′ (TK13), and 5′-ACACCTATGAACCACAAGGAC-3′ (TK30). The CCL25-deficient mice were kept under specific pathogen-free conditions and back-crossed 15 times on a C57BL/6N background.

Multicolor flow cytometry analysis

Six-color flow cytometry was performed on mice between 4 and 12 wk of age as described (6). Cell suspensions were prepared from WT, CCL25-deficient, and CCR9-deficient thymus, spleen (SPL), mesenteric lymph nodes (MLN), peripheral lymph nodes (PLN), Peyer's patches (PP), lamina propria (LP lymphocyte (LPL)), and epithelium (intraepithelial lymphocytes (IEL)) of the small intestine. We used directly conjugated mAbs (CD4, CD8, CD44, TCRβ, TCR$\gamma\delta$, Vα2, Vβ5, and mouse IgG2a isotype control) from BD Biosciences (CD4, CD8, CD45.1, and CD45.2) from eBioscience polyclonal second-stage Ab (Cy2 Goat anti-mouse IgG Fcγ) from Jackson ImmunoResearch Laboratories and unconjugated anti-CCR9 mAb (clone CW-1.2 generated in our laboratory (6)). Cytometry was acquired on dual-laser MoFlo cytometer (DakoCytomation) configured for six colors: 1, FITC; 2, PE; 3, PE-Texas Red; 4, PE-Cy7; 5, Cy5; 6, allophycocyanin-Cy7, and analyzed using FlowJo software (FlowJo).

PP and LPL isolation

PP and LPLs were isolated as previously described (22). In brief, small intestines were harvested, and flushed with PBS. PP were then removed; the gut was opened longitudinally and then cut in 0.5-cm pieces. PP and intestinal pieces were incubated (separately) in 1× PBS plus 3 mM BSA, 2 × 10 min at 37°C, and then placed in RPMI 1640 plus 1% dialyzed FCS plus 1 mM EGTA plus 1.5 mM $MgCl_2$ for 2 × 15 min at 37°C to remove IEL and all epithelial cells. PP and intestinal pieces were then digested in RPMI 1640 plus 20% FCS plus 100 U/ml collagenase (type VIII; Sigma-Aldrich) plus 5 μg/ml DNase (Sigma-Aldrich) for 90 min at 37° C. LPL were further purified on a Ficoll-Paque gradient (Amersham Biosciences) and stained with mAbs for flow cytometry.

IEL isolation and histological studies

IEL from the small intestine were isolated as previously described (23). In brief, PP were removed and, after flushing with PBS, the gut was opened on a wet square of Optima fabric (Allegiance Healthcare). The mucosa was scraped with a scalpel and then dissociated by stirring in 50 ml of medium 199 containing 10% newborn calf serum and DTT (1 mM) for 15 min at room temperature. After centrifugation, the pellet was resuspended in PBS containing 10% newborn calf serum, vortexed for 3 min, and rapidly passed through a glass wool column

(1.6 g packed in a 20-ml syringe; Fisher Scientific). IEL were further purified on a Ficoll-Paque gradient and stained with mAbs for flow cytometry analysis. For histological studies, a 1-cm piece of small intestine, taken 3 cm below the pylorus, was properly oriented on filter paper and fixed in Carnoy's fluid for 24 h. Paraffin-embedded sections were prepared and stained with periodic-acid Schiff and hematoxylin.

Adoptive transfer

OT-1-Tg mice (24) were bred onto CD45.1$^+$ C57BL/6N mice (B6.SJL-*Ptprc*^{a} *Pep3*^{b}/BoyJ; The Jackson Laboratory). Splenocytes were then obtained from CD45.1$^+$ OT-1-Tg donor mice. A total of 5×10^6 naive CD8$^+$ OT-1-Tg donor cells were adoptively transferred by i.v. injection into recipient mice (C57BL/6N, CCL25-deficient, or CCR9-deficient mice). Mice were sensitized orally or i.p. 24 h after transfer with 10 μg of cholera toxin (CT; Calbiochem) or 10 μg of CT together with 5 mg of OVA (Sigma-Aldrich) and subsequently harvested 4 days after sensitization.

Results

We generated a novel strain of mice lacking the gene for chemokine CCL25 (Fig. 1). These mice were viable, fertile, and without gross morphologic or developmental abnormalities. The strain was kept under SPF conditions and backcrossed 15 times onto the C57BL/6 background for our experiments.

Thymic phenotype of CCL25$^{-/-}$ mice

We first assessed whether the absence of CCL25 had an impact on the cell surface expression of CCR9. For that purpose, we used an anti-CCR9 mAb to analyze T cells at various developmental stages. Fig. 2*A* shows the profiles obtained with thymocytes isolated from WT, CCL25$^{-/-}$, and CCR9$^{-/-}$ mice. As we have shown previously, CCR9 was expressed at high levels by the vast majority of WT mouse thymocytes, and as expected, was absent from CCR9$^{-/-}$ thymocytes (6). Interestingly, CCL25$^{-/-}$ thymocytes expressed CCR9 at >1.5-fold higher levels than WT thymocytes ($p < 0.05$, see Fig. 2*A*, *legend*).

We next examined the relative composition of thymocytes according to the four major subsets: double negative (DN), double positive (DP), CD4 single positive (SP), and CD8SP (Fig. 3*A*). Thymic size and cellularity were comparable among WT, CCR9$^{-/-}$, and CCL25$^{-/-}$ mice. As we reported previously (6,16), there were no differences in the relative proportions of these subsets between normal and CCR9-deficient mice (Fig. 3*A*). This was also the case for CCL25-deficient mice. Thus, there were no appreciable differences in the relative percentages of DN, DP, CD4SP, and CD8SP subsets among the three mouse strains.

Phenotype of lymphoid organs from CCL25$^{-/-}$ mice

We previously showed that CCR9 is expressed by essentially all naive CD8 T cells found in WT mice (Fig. 2*B* and Ref. 6). This was also the case for CCL25$^{-/-}$ mice (Fig. 2*B*). CCR9 was not expressed by naive CD4 T cells (Fig. 2*B* and Ref. 6). Expression of CCR9 by naive CD8 T cells is also seen in the MLN (Fig. 2*C*): CD44^{low} naive CD8 populations from the WT and CCL25$^{-/-}$ MLN are CCR9^{low}, but as expected, those from the CCR9$^{-/-}$ MLN are CCR9^{neg}.

The memory-phenotype (CD44^{high}) populations of both CD4 and CD8 T cells from WT mice contained CCR9^{high} subsets predisposed to small intestinal homing (Fig. 2 and Ref. 13). WT and CCL25$^{-/-}$ MLN contained similar proportions of CCR9^{high} memory-phenotype cells (Fig. 2*C*). In addition to naive and CCR9^{high} memory cells, there was also a population of CCR9^{neg} memory-phenotype cells present in MLN (Fig. 2*C*). This population is likely to

contain nonintestinal memory T cells and/or intestinal memory T cells specific for the colon (where CCL25 is poorly expressed (2)).

Intestinal phenotype in CCL25$^{-/-}$ mice

We next examined the lymphocyte populations residing within in the small intestine itself. We assessed the total number of IEL by counting the number of IEL in duodenal tissue sections and calculating the ratio of IEL to epithelial cells (EC) (16,22). We found that the total number of IEL present in CCL25$^{-/-}$ mice was dramatically and significantly lower than WT mice, but similar CCR9$^{-/-}$ mice (Fig. 3*B* and Ref. 16).

Consistent with earlier findings in CCR9$^{-/-}$ mice (16), the significant reduction in total IEL appeared to be primarily due to a reduction in TCR$\gamma\delta^{+}$ rather than TCR$\alpha\beta^{+}$ cells, although the difference did not reach statistical significance (Fig. 3*C*). TCR$\gamma\delta^{+}$ cells normally constitute the majority of IEL, but only accounted for 20 –30% of the total IEL T cell population in CCR9$^{-/-}$ and CCL25$^{-/-}$ mice (Fig. 3*C*, □). The apparent reduction in TCRγ δ representation shown in Fig. 3*C*, together with the absolute numerical loss of IEL shown in Fig. 3*B*, constituted a 5- to 6-fold reduction in total TCR$\gamma\delta^{+}$ IEL. Interestingly, the loss of TCR$\gamma\delta^{+}$ cells from the intestinal epithelium was accompanied by an increased relative percentage of TCR$\gamma\delta^{+}$ cells in the MLN (Fig. 3*E*). This is consistent with the notion that TCR$\gamma\delta^{+}$ cells excluded from the intestinal epithelium accumulated in the MLN.

LPL subsets have not been previously examined in either CCL25$^{-/-}$ or CCR9$^{-/-}$ mice. It is not possible to assess the absolute number of lymphocytes in the LP as was done for the epithelium in Fig. 3*B*. This is because the histology of the epithelium (unlike the LP) uniquely provides us with an “internal control” (i.e., the epithelial cells) with which to calculate an IEL:EC ratio. Regardless of this limitation, we found that the proportion of CD8 T lymphocytes was significantly reduced in the LPL populations of both CCR9$^{-/-}$ and CCL25$^{-/-}$ mice (Fig. 3*D*). The relative loss of CD8 T cells in LP was accompanied by a relative increase in CD4 T cells (Fig. 3*D*) and B cells (M.-A. Wurbel and J. J. Campbell, unpublished data).

We next examined CCR9 expression by flow cytometry for the major T cell subsets of the epithelial and LP compartments. As in WT mice, essentially all IEL populations from CCL25-deficient mice expressed CCR9 (Fig. 4). In contrast, CCR9 expression differed between WT and CCL25$^{-/-}$ LPL, as the vast majority of CD4^{+} and CD8^{+} T cells from WT mice expressed CCR9, whereas significant numbers of CCR9^{neg} T cells were present in CCL25$^{-/-}$ LPL (Fig. 4).

OT-1 adoptive-transfer model

To assess the ability of naive T cells to differentiate into CCR9^{high} memory cells within CCL25$^{-/-}$ hosts, we next established an adoptive transfer assay using TCR-Tg OT-1 splenocytes from naive donors. We have previously used a similar system to study the role of another chemokine receptor, CCR4, in skin-specific homing of TCR-Tg OT-2 cells (25). CD8 T cells from TCR-Tg OT-1 mice recognize an OVA peptide corresponding to amino acid 257–264 in the context of the H-2K^{b} MHC class I molecule (24). After reconstitution, hosts were treated orally by gavage containing adjuvant alone (adjuvant = CT) or whole OVA protein with adjuvant. Four days after oral sensitization, lymphocytes were harvested from blood, SPL, MLN, PP, small intestinal LP, and small intestinal epithelium. Donor OT-1 cells were CD45.1$^{+/+}$, while the hosts were CD45.2$^{+/+}$, allowing us to distinguish between the donor and host cells within the harvested populations.

We first assessed the differentiation of naive OT-1 cells into CCR9^{high} memory-phenotype cells within WT hosts. Following oral sensitization with OVA plus CT, memory-phenotype

OT-1 cell numbers in the MLN reached a peak at day 4 (M.-A. Wurbel and J. J. Campbell, unpublished data). When we gated on total memory-phenotype CD8 T cells from MLN of OVA plus CT-treated hosts at day 4 after treatment, roughly 20% were derived from the OT-1 donor (Fig. 5*A*). This number was dramatically greater increased over hosts treated with CT only (Fig. 5*A*). When T cells from MLN were gated donor-derived OT-1 cells, nearly 50% had differentiated into "small intestine-tropic memory T cells" that are characterized by a $CD44^{high}/CCR9^{high}$ phenotype (Fig. 5*A*). In contrast, donor cells from hosts treated with CT only retained a $CD44^{low}/CCR9^{low}$ "naive" phenotype (Fig. 5*A*, *bottom row*, *middle panel*).

OT-1 cells in CCL25-deficient hosts

We next asked whether $CCR9^{high}$ memory-phenotype OT-1 cells could be generated within the MLN of $CCL25^{-/-}$ hosts (Fig. 5*B*). $CCR9^{-/-}$ hosts were also studied as an additional control. We did not find any significant difference in the ability of OT-1 cells to differentiate into the $CCR9^{high}$ memory-phenotype within WT, $CCL25^{-/-}$, or $CCR9^{-/-}$ hosts to after OVA plus CT treatment (Fig. 5*B*, *lower panel*), nor into the memory-phenotype in general (Fig. 5*B*, *upper panel*) within the MLN. Therefore, it can be concluded that administration of oral Ag caused naive OT-1 cells to differentiate into $CCR9^{high}$ memory-phenotype CD8 T cells in the MLN, whether or not the host mice posses a functional *CCL25* gene. These oral Ag-induced $CCR9^{high}$ memory-phenotype cells expressed normal levels of integrin proteins associated with intestinal homing, including α_4, β_7, and α_E (CD103), demonstrating that these cells truly possess the full "gut-homing" phenotype (Fig. 5*C*).

Oral vs i.p. immunization routes

As i.p. injection of Ag has often been used as a model for intestinal inflammation, we compared this route of Ag exposure do the direct oral route used above. We examined the memory phenotype (CD44 level) and gut phenotype (CCR9 expression) of OT-1 cells in the PLN and MLN of mice treated via these different routes (Fig. 6). Unlike MLN-derived OT-1 cells from orally treated hosts (which primarily displayed the gut memory phenotype), the vast majority of those from i.p.-treated hosts displayed the $CD44^{high}/CCR9^{neg}$ "systemic memory" phenotype.

We further investigated differences resulting from these different immunization routes by examining PLN, which are not associated with gut inflammation. Most of the PLN-derived OT-1 cells resulting from oral immunization remained of the naive phenotype. In dramatic contrast, essentially all PLN-derived OT-1 cells resulting from i.p. immunization were of the memory phenotype, with the vast majority lacking CCR9. Thus, i.p. immunization appears to cause a severe, generalized proliferation of systemic memory-phenotype cells throughout the organism (including the gut-associated lymphoid tissues (GALT)). In contrast, the identical immunogen given through the oral route causes differentiation of intestinal-memory cells and is primarily restricted to the gut and the GALT.

Trafficking to the small intestine

We next asked whether the "small intestine-tropic" memory-phenotype CD8 T cells generated within CCL25-deficient hosts were capable of homing to the CCL25-deficient small intestine. After careful removal of PP, LPL, and IEL were separately isolated at day 4 postsensitization. We found that OT-1 cells accumulated >10-fold better within LP (Fig. 7*A*) and epithelium (Fig. 7*B*) in response to OVA plus CT than to adjuvant alone.

For $CCL25^{-/-}$ recipients, the number of OT-1 donor cells was significantly and dramatically decreased in both LP and epithelium of $CCL25^{-/-}$ recipients (Fig. 7, *A* and *B*). OT-1 cells within $CCR9^{-/-}$ recipients (which express normal amounts of CCL25) were not significantly different from those of WT recipients (Fig. 7, *A* and *B*).

We next asked whether the increased percentage of OT-1 cells in the small intestine induced by oral Ag was organ specific, or instead reflected a generalized increase in OT-1 numbers throughout the body. Pairs of mice were treated in parallel, with one member of each pair receiving OVA plus CT immunization and the other receiving CT only. Thus, for each pair, we could calculate the OVA-specific fold-increase in OT-1 cells within various organs (Fig. 8).

We found that the fold-increase in OT-1 donor cell representation was 50-fold for LPL and 150-fold for IEL in WT hosts (Fig. 8*A*). Within the lymphoid organs, we found that the PP had the highest Ag-induced increase in OT-1 cells (Fig. 8, *insets*). In CCL25$^{-/-}$ hosts, the response was dramatically reduced, but this smaller response remained specific to the intestine. The response in CCR9$^{-/-}$ hosts was not significantly different from that of WT hosts.

Discussion

We have developed a CCL25$^{-/-}$ mouse strain to assess the role of CCL25-CCR9 interactions during T cell-mediated gut-specific immunological responses. We first characterized the phenotype of these mice and then used them to demonstrate that CCL25 is an indispensable component of Ag-specific T cell homing to the LP and epithelium of the small intestine.

In characterizing CCL25$^{-/-}$ thymocytes, we found an interesting difference in CCR9 expression between the WT and the CCL25$^{-/-}$ mice. CCL25$^{-/-}$ thymocytes expressed significantly more cell surface CCR9 (>1.5 times) than thymocytes from WT mice (Fig. 2*A*). This difference could possibly reflect a constant presence of CCL25 within WT thymus, causing partial internalization of CCR9. This process would be absent from the CCL25$^{-/-}$ thymus. In support of this hypothesis, when thymocytes were isolated, washed, and incubated at 37°C, cell surface CCR9 expression was significantly increased by WT but not CCL25$^{-/-}$ thymocytes (M.-A. Wurbel and J. J. Campbell, unpublished data). The increase in cell surface CCR9 expression seen in the CCL25$^{-/-}$ thymus was not seen in CCL25$^{-/-}$ secondary lymphoid organs. This implies that WT splenocytes and lymph node cells are not exposed to the "CCR9-internalizing levels" of CCL25 that we propose to be present in the thymus (see below).

There were no significant differences observed among WT, CCR9$^{-/-}$, and CCL25$^{-/-}$ thymocytes regarding the four major subsets (DN, DP, CD4SP, and CD8SP). However, we and others have shown that the apparent lack of thymic phenotype for CCR9$^{-/-}$ mice is misleading (6,12), which is probably also the case for CCL25$^{-/-}$ mice. This is because a very important component of normal lymphocyte trafficking, i.e., competition (26) for limited microenvironmental niches between CCR9^{+} and CCR9^{-} thymocyte populations, is missing in CCR9$^{-/-}$ mice. In fact, CCR9$^{-/-}$ BM cells are 10- to 15-fold less likely to develop into mature T cells when equal numbers of CCR9$^{+/+}$ competitor BM cells are present (6,10,12).

In the small intestine, CCL25$^{-/-}$ mice have a significant reduction in absolute IEL count as measured by lymphocyte-epithelial cell ratio, similar to that previously observed for CCR9$^{-/-}$ mice (Fig. 3*B* and Ref. 16). This reduction is focused primarily on the TCR$\gamma\delta^{+}$ subset, which normally accounts for the majority of IEL (Fig. 3*C*). The relative proportion of TCR$\alpha\beta$ T cells was increased, showing that absence of CCL25-CCR9 interaction had its most profound effect on the $\gamma\delta$ population under SPF conditions. We estimate the reduction in absolute number of TCR$\gamma\delta$ IEL to be 5-to 6-fold (Fig. 3, *B* and *C*), and somewhat lower for the $\alpha\beta$ population. Interestingly, those few TCR$\gamma\delta^{+}$ IEL found in CCL25$^{-/-}$ epithelium express CCR9 at normal levels (Fig. 4*B*). This population might result from local intestinal development/maturation rather than homing of thymus-derived cells to the epithelium (i.e., thymo-independent IEL).

The decreased relative percentage of TCR$\gamma\delta$ cells in CCL25$^{-/-}$ IEL was accompanied by an increased relative percentage of TCR$\gamma\delta$ cells in the MLN and SPL (Fig. 3*E*), a phenomenon also seen in CCR9$^{-/-}$ mice (16). This suggests that many TCR$\gamma\delta$ cells are excluded from the small intestine by the absence of CCL25-CCR9 interactions, and therefore accumulate in lymphoid organs. This is consistent with our finding that the vast majority of TCR$\gamma\delta$ cells express CCR9 in the MLN of both WT and CCL25$^{-/-}$ mice (M.-A. Wurbel and J. J. C., unpublished data).

LPL populations have not been previously examined in CCL25$^{-/-}$ or CCR9$^{-/-}$ mice. In this study, we found that the proportion of CD8^{+} T cells was significantly reduced in LPL of CCL25$^{-/-}$ AND CCR9$^{-/-}$ strains when compared with WT LPL (Fig. 3*D*). These data are consistent with the notion that CCL25-CCR9 interactions are important for the homing of CD8 T cells to both the epithelium and to the LP of the small intestine.

Consistent with the above finding, the proportion of CD4^{+} and CD8^{+} LPL expressing CCR9 was significantly reduced in LP of CCL25$^{-/-}$ mice (Fig. 4*A*). CCR9^{neg} T cells were rare in WT LP, but constituted up to a third of T cells in CCL25$^{-/-}$ LP. This finding is congruent with the notion that CCR9^{+} T cells are more efficient than CCR9^{neg} T cells at homing to the LP in WT mice. This competitive advantage would no longer be relevant in the absence of CCL25, allowing a greater proportion of CCR9^{neg} cells to enter the LP in CCL25$^{-/-}$ mice.

After addressing the development and homeostasis of lymphocyte subsets within CCL25$^{-/-}$ mice under SPF and steady-state conditions, we next assessed the generation of Ag-specific immunological responses within the CCL25-deficient intestine. For that purpose, we developed an adoptive transfer model in which naive CD8 T cells from the TCR-Tg OT-1 (24) mouse strain were introduced into CCL25$^{-/-}$ hosts.

This approach allowed us to monitor a naive TCR-Tg CD8 T cell population as it acquired tissue-specific homing properties within the adoptive host. This model system recapitulated the physiological conditions under which a small number of Ag-specific lymphocytes must compete with a vastly larger population of nonspecific lymphocytes to accumulate within a given tissue. Because our focus was on intestinal immunity, we chose an immunization route in which Ag was applied directly to the intestinal lumen.

The differentiation of naive CD8 T cells into gut-tropic memory cells in vivo requires presentation of cognate Ag by intestine-derived dendritic cells (17,27). Recent evidence suggests that retinoic acid is a component of the signaling mechanism by which naive CD8 T cells are induced to express high levels of CCR9 (28). It was not known, however, whether the signaling through CCR9 (presumably via CCL25) was necessary to generate CCR9^{high} memory cells in vivo. This is an especially interesting question for naive murine CD8 T cells, which express functional CCR9 (although at levels ~10-fold lower that intestinal memory CD8 T cells (6)), and therefore have the means to receive a potential CCL25-mediated differentiation signal.

Our assay showed that Ag-driven generation of CCR9^{high} memory CD8^{+} T cells was CCL25 independent. Application of luminal Ag induced CCR9^{high} memory differentiation for more than half of all OT-1 cells in the MLN, regardless of whether the host was WT, CCL25$^{-/-}$, or CCR9$^{-/-}$. These cells also expressed the integrin proteins known to be involved in homing to the intestine (i.e. α_4, β_7, and α_E (Fig. 5*C*)). We did not observe induction of CCR9^{neg} memory cells, which are more common than CCR9^{high} memory cells in most lymphoid organs (for example, see the steady-state distribution of WT memory cells in Fig. 2*C*).

Interestingly, the luminal route of Ag exposure was important for this specificity (Fig. 6). A different immunization route commonly used to induce intestinal inflammation, i.p. injection,

caused OT-1 cells to differentiate primarily into $CCR9^{neg}$ systemic-memory phenotype OT-1 cells. Unlike oral immunization, i.p. immunization generated few $CCR9^{high}$ intestinal-memory phenotype OT-1 cells. Large numbers of $CCR9^{neg}$ memory-phenotype OT-1 cells were found in all lymphoid organs tested after i.p. immunization, including PLN. Most of the OT-1 cells in the PLN after oral immunization remained in the naive phenotype. Taken together, these findings suggest that i.p. immunization causes a widely disseminated systemic response and constitutes a very poor model for gut-specific immune responses.

The most important question addressed by this study was the necessity for CCL25 in homing of gut-tropic, Ag-specific CD8 T cells to the small intestine. A definitive answer to this question could shed light on whether pharmacological interference with CCL25-CCR9 interactions could provide useful treatments in human disease.

We found that OT-1 cells were profoundly impaired at homing to the small intestine of $CCL25^{-/-}$ mice. This impairment was dramatic and significant in both the LP and epithelial compartments. Although it has been shown that CCL25 transcripts are limited mainly to the epithelial cells that line the small intestine (2), the literature remains conflicted as to whether CCR9 protein is also limited to the epithelium (13) or rather is present in both the epithelium and the LP (29). Our data unambiguously demonstrate that CCL25 has an influence on lymphocyte trafficking to both compartments.

It should be noted that the profound reduction of OT-1 accumulation in the $CCL25^{-/-}$ small intestine was truly a defect and not merely a temporal delay. The peak of Ag-specific OT-1 accumulation was at day 4 for WT, $CCR9^{-/-}$, and $CCL25^{-/-}$ hosts. The accumulation did not increase within LP or epithelium on days 5, 6, 7, 8, or 10 (day 10 was the latest time point tested; M.-A. Wurbel and J. J. Campbell, unpublished data).

We have eliminated a potentially confounding issue in comparing OT-1 intestinal homing between WT and $CCL25^{-/-}$ hosts, by also studying the $CCR9^{-/-}$ hosts. As steady-state intestinal lymphocyte populations were different between WT and $CCL25^{-/-}$ mice, this could mean that immunologically relevant microenvi-ronments were abnormal in the $CCL25^{-/-}$ intestine. The defect in OT-1 accumulation might therefore have been secondary to such differences in the intestinal parenchyma, rather than a direct effect on OT-1 trafficking. However, $CCR9^{-/-}$ intestines are histologically identical with $CCL25^{-/-}$ intestines, except that they produce normal amounts of CCL25. We found no significant difference in OT-1 homing between the WT and $CCR9^{-/-}$ intestine, but a profound difference between the $CCR9^{-/-}$ and $CCL25^{-/-}$ intestine. This strongly supports the conclusion that CCL25 is necessary for homing of Ag-specific OT-1 cells to the small intestine.

References

1. Vicari AP, Figueroa DJ, Hedrick JA, Foster JS, Singh KP, Menon S, Copeland NG, Gilbert DJ, Jenkins NA, Bacon KB, Zlotnik A. TECK: a novel CC chemokine specifically expressed by thymic dendritic cells and potentially involved in T cell development. Immunity 1997;7:291–301. [PubMed: 9285413]
2. Wurbel MA, Philippe JM, Nguyen C, Victorero G, Freeman T, Wooding P, Miazek A, Mattei MG, Malissen M, Jordan BR, et al. The chemokine TECK is expressed by thymic and intestinal epithelial cells and attracts double- and single-positive thymocytes expressing the TECK receptor CCR9. Eur J Immunol 2000;30:262–271. [PubMed: 10602049]
3. Zabel BA, Agace WW, Campbell JJ, Heath HM, Parent D, Roberts AI, Ebert EC, Kassam N, Qin S, Zovko M, et al. Human G protein-coupled receptor GPR-9 – 6/CC chemokine receptor 9 is selectively expressed on intestinal homing T lymphocytes, mucosal lymphocytes, and thymocytes and is required for thymus-expressed chemokine-mediated chemotaxis. J Exp Med 1999;190:1241–1256. [PubMed: 10544196]

4. Benz C, Heinzel K, Bleul CC. Homing of immature thymocytes to the subcapsular microenvironment within the thymus is not an absolute requirement for T cell development. Eur J Immunol 2004;34:3652–3663. [PubMed: 15484191]
5. Uehara S, Hayes SM, Li L, El-Khoury D, Canelles M, Fowlkes BJ, Love PE. Premature expression of chemokine receptor CCR9 impairs T cell development. J Immunol 2006;176:75– 84. [PubMed: 16365398]
6. Wurbel MA, Malissen B, Campbell JJ. Complex regulation of CCR9 at multiple discrete stages of T cell development. Eur J Immunol 2006;36:73– 81. [PubMed: 16342233]
7. Norment AM, Bogatzki LY, Gantner BN, Bevan MJ. Murine CCR9, a chemokine receptor for thymus-expressed chemokine that is up-regulated following pre-TCR signaling. J Immunol 2000;164:639–648. [PubMed: 10623805]
8. Scimone ML, Aifantis I, Apostolou I, von Boehmer H, von Andrian UH. A multistep adhesion cascade for lymphoid progenitor cell homing to the thymus. Proc Natl Acad Sci USA 2006;103:7006–7011. [PubMed: 16641096]
9. Schwarz BA, Bhandoola A. Trafficking from the bone marrow to the thymus: a prerequisite for thymopoiesis. Immunol Rev 2006;209:47–57. [PubMed: 16448533]
10. Schwarz BA, Sambandam A, Maillard I, Harman BC, Love PE, Bhandoola A. Selective thymus settling regulated by cytokine and chemokine receptors. J Immunol 2007;178:2008–2017. [PubMed: 17277104]
11. Liu C, Ueno T, Kuse S, Saito F, Nitta T, Piali L, Nakano H, Kakiuchi T, Lipp M, Hollander GA, Takahama Y. The role of CCL21 in recruitment of T-precursor cells to fetal thymi. Blood 2005;105:31–39. [PubMed: 15358618]
12. Uehara S, Grinberg A, Farber JM, Love PE. A role for CCR9 in T lymphocyte development and migration. J Immunol 2002;168:2811–2819. [PubMed: 11884450]
13. Kunkel EJ, Campbell JJ, Haraldsen G, Pan J, Boisvert J, Roberts AI, Ebert EC, Vierra MA, Goodman SB, Genovese MC, et al. Lymphocyte CC chemokine receptor 9 and epithelial thymus-expressed chemokine (TECK) expression distinguish the small intestinal immune compartment: epithelial expression of tissue-specific chemokines as an organizing principle in regional immunity. J Exp Med 2000;192:761–768. [PubMed: 10974041]
14. Papadakis KA, Prehn J, Moreno ST, Cheng L, Kouroumalis EA, Deem R, Breaverman T, Ponath PD, Andrew DP, Green PH, et al. CCR9-positive lymphocytes and thymus-expressed chemokine distinguish small bowel from colonic Crohn's disease. Gastroenterology 2001;121:246–254. [PubMed: 11487533]
15. Papadakis KA, Prehn J, Nelson V, Cheng L, Binder SW, Ponath PD, Andrew DP, Targan SR. The role of thymus-expressed chemokine and its receptor CCR9 on lymphocytes in the regional specialization of the mucosal immune system. J Immunol 2000;165:5069–5076. [PubMed: 11046037]
16. Wurbel MA, Malissen M, Guy-Grand D, Meffre E, Nussenzweig MC, Richelme M, Carrier A, Malissen B. Mice lacking the CCR9 CC-chemokine receptor show a mild impairment of early T- and B-cell development and a reduction in T-cell receptor $\gamma\delta^+$ gut intraepithelial lymphocytes. Blood 2001;98:2626–2632. [PubMed: 11675330]
17. Johansson-Lindbom B, Svensson M, Wurbel MA, Malissen B, Marquez G, Agace W. Selective generation of gut tropic T cells in gut-associated lymphoid tissue (GALT): requirement for GALT dendritic cells and adjuvant. J Exp Med 2003;198:963–969. [PubMed: 12963696]
18. Staton TL, Habtezion A, Winslow MM, Sato T, Love PE, Butcher EC. $CD8^+$ recent thymic emigrants home to and efficiently repopulate the small intestine epithelium. Nat Immunol 2006;7:482–488. [PubMed: 16582913]
19. Staton TL, Johnston B, Butcher EC, Campbell DJ. Murine $CD8^+$ recent thymic emigrants are α_E integrin-positive and CC chemokine ligand 25 responsive. J Immunol 2004;172:7282–7288. [PubMed: 15187103]
20. Kress C, Vandormael-Pournin S, Baldacci P, Cohen-Tannoudji M, Babinet C. Nonpermissiveness for mouse embryonic stem (ES) cell derivation circumvented by a single backcross to 129/Sv strain: establishment of ES cell lines bearing the Omd conditional lethal mutation. Mamm Genome 1998;9:998–1001. [PubMed: 9880667]

21. Schwenk F, Baron U, Rajewsky K. A cre-transgenic mouse strain for the ubiquitous deletion of loxP-flanked gene segments including deletion in germ cells. Nucleic Acids Res 1995;23:5080–5081. [PubMed: 8559668]

22. Arstila T, Arstila TP, Calbo S, Selz F, Malassis-Seris M, Vassalli P, Kourilsky P, Guy-Grand D. Identical T cell clones are located within the mouse gut epithelium and lamina propria and circulate in the thoracic duct lymph. J Exp Med 2000;191:823–834. [PubMed: 10755885]

23. Guy-Grand D, Griscelli C, Vassalli P. The mouse gut T lymphocyte, a novel type of T cell: nature, origin, and traffic in mice in normal and graft-versus-host conditions. J Exp Med 1978;148:1661–1677. [PubMed: 31410]

24. Hogquist KA, Jameson SC, Heath WR, Howard JL, Bevan MJ, Carbone FR. T cell receptor antagonist peptides induce positive selection. Cell 1994;76:17–27. [PubMed: 8287475]

25. Campbell JJ, O'Connell DJ, Wurbel MA. Cutting edge: chemokine receptor CCR4 is necessary for antigen-driven cutaneous accumulation of CD4 T cells under physiological conditions. J Immunol 2007;178:3358–3362. [PubMed: 17339428]

26. Baekkevold ES, Wurbel MA, Kivisakk P, Wain CM, Power CA, Haraldsen G, Campbell JJ. A role for CCR4 in development of mature circulating cutaneous T helper memory cell populations. J Exp Med 2005;201:1045–1051. [PubMed: 15795234]

27. Mora JR, Bono MR, Manjunath N, Weninger W, Cavanagh LL, Rosemblatt M, Von Andrian UH. Selective imprinting of gut-homing T cells by Peyer's patch dendritic cells. Nature 2003;424:88–93. [PubMed: 12840763]

28. Mora JR, von Andrian UH. Retinoic acid: an educational "vitamin elixir" for gut-seeking T cells. Immunity 2004;21:458–460. [PubMed: 15485623]

29. Hosoe N, Miura S, Watanabe C, Tsuzuki Y, Hokari R, Oyama T, Fujiyama Y, Nagata H, Ishii H. Demonstration of functional role of TECK/CCL25 in T lymphocyte-endothelium interaction in inflamed and uninflamed intestinal mucosa. Am J Physiol 2004;286:G458–G466.

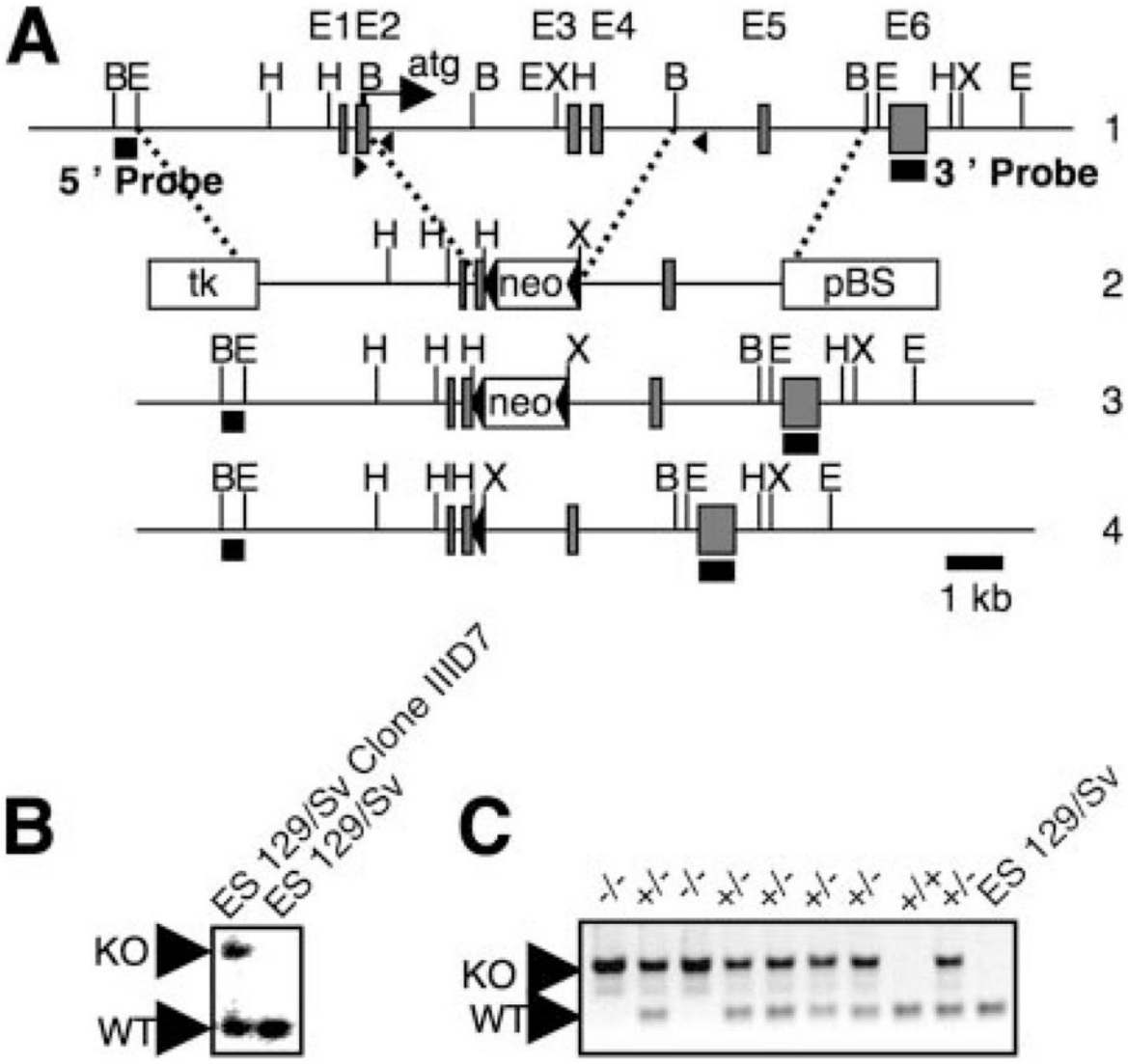

Figure 1.

Generation and identification of CCL25-deficient mice. *A*, 1) Partial restriction map of the WT *CCL25* gene. Exons 1– 6 are shown as gray boxes. The restriction sites are B (*Bgl*II), E (*Eco*R V), H (*Hin*dIII), and X (*Xba*I) (2). Targeting vector used for the deletion of the 3′ end of exon 2 (starting at the *Bgl*II restriction site and including ATG), exon 3 and exon 4 (containing the four cysteine residues crucial for the folding of CCL25). One diagnostic *Xba*I restriction site was introduced at the 5′ end of the loxP-flanked neomycin resistance gene (neo), whereas a diagnostic *Bgl*II restriction site was lost in exon 2. □, Correspond to the thymidine kinase expression cassette (tk), to the loxP-flanked neomycin gene, and to the pBluescript IIKS$^+$ vector (pBS) (3). Structure of the targeted allele following homologous recombination (4). Final structure of the targeted allele after removal of the neomycin-resistance gene via Cre-mediated recombination with Cre Deleter mice. ■, The 5′ and 3′ single-copy probes used to verify the targeting events; the position of the primers used to monitor the germline transmission of the intended mutation are indicated by arrows. *B*, Southern blot analysis of the rES cell clone IIID7 that gave germline transmission before deletion of the neomycin-resistance gene. DNA was digested with *Bgl*II and hybridized with the 5′ single copy probe. *C*, DNA-

PCR analysis of wild-type (+/+), neomycin-deleted heterozygous (+/−), and neomycin-deleted homozygous (−/−) littermates using the pair of primers shown in *A*. Targeted *CCL25* allele gave an amplified PCR product of 510 bp, whereas the wild-type allele gave an amplified PCR product of 280 bp. Amplified products were run on an agarose gel and stained with ethidium bromide.

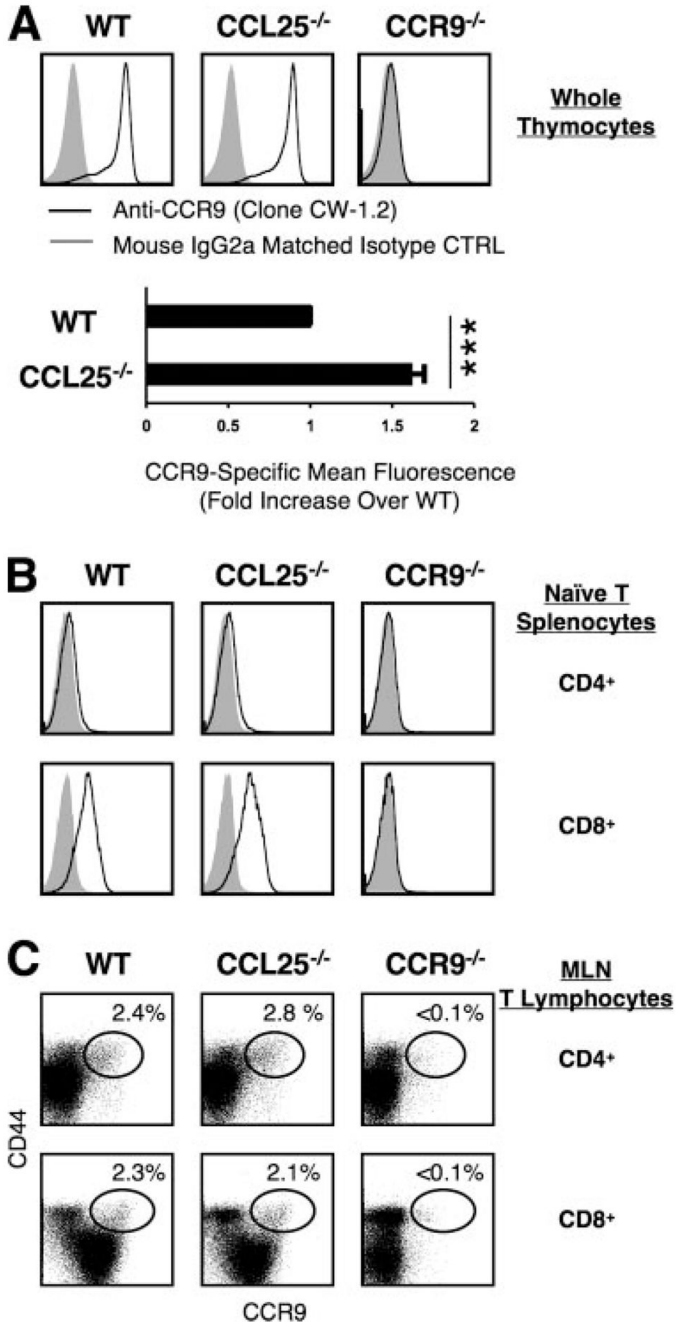

Figure 2.

CCR9 expression by thymocytes and mature lymphocytes from WT and CCL25-deficient mice. *A* and *B*, Cells from thymus and SPL of WT, CCL25$^{-/-}$, and CCR9$^{-/-}$ mice were stained and analyzed by flow cytometry. CCR9 cell surface expression was assessed by mAb CW-1.2 (black lines) and overlaid on isotype-matched mIgG$_{2a}$ control (gray filled curves). *A*, *Upper panels*, CCR9 expression on unfractionated thymocytes (gated only by scatter). *Lower panel*, CCL25-deficient thymocytes expressed CCR9 >1.5-fold more brightly (by mean fluorescence) than WT thymocytes (***, $p < 0.05$ in a Wilcoxon-signed rank, $n = 5$). *B*, *Upper panels*, CCR9 expression by CD4^{+} naive T splenocytes (gated as CD4$^{+/}$B220^{-}/CD44^{low}/CD45RB^{high} lymphocytes). No significant CCR9 expression was observed for any of the three genotypes.

Bottom row, CCR9 expression by $CD8^+$ naive T splenocytes (gated as $CD3\varepsilon^{+/}CD8^{+/}CD44^{low}/PNA^{low}$ lymphocytes). CCR9 expression was not significantly different between WT and $CCL25^{-/-}$ mice. *C*, CD44 vs CCR9 expression on $CD4^+$ and $CD8^+$ T cells from MLN of WT, $CCL25^{-/-}$, and $CCR9^{-/-}$ mice. *Top row*, Staining of $CD4^+$ T cells (gated as $CD4^+/B220^-$ lymphocytes). There was no significant difference in the representation of $CD44^{high}/CCR9^{high}$ memory cells between WT and $CCL25^{-/-}$ MLN within the $CD4^+$ population. *Bottom row*, Staining of $CD8^+$ T cells (gated as $CD3\varepsilon^{+/}CD8^+$ lymphocytes). There was no significant difference in the representation of $CD44^{high}/CCR9^{high}$ memory cells between WT and $CCL25^{-/-}$ MLN within the $CD8^+$ population. It should also be noted that this staining protocol also highlights the fact that $CD44^{low}$ naive CD8 T cells are clearly $CCR9^{low}$ in the WT and $CCL25^{-/-}$ MLN, but are $CCR9^{neg}$ in the $CCR9^{-/-}$ MLN. All flow cytometry panels in this figure depict individual experiments and represent more than five repeats.

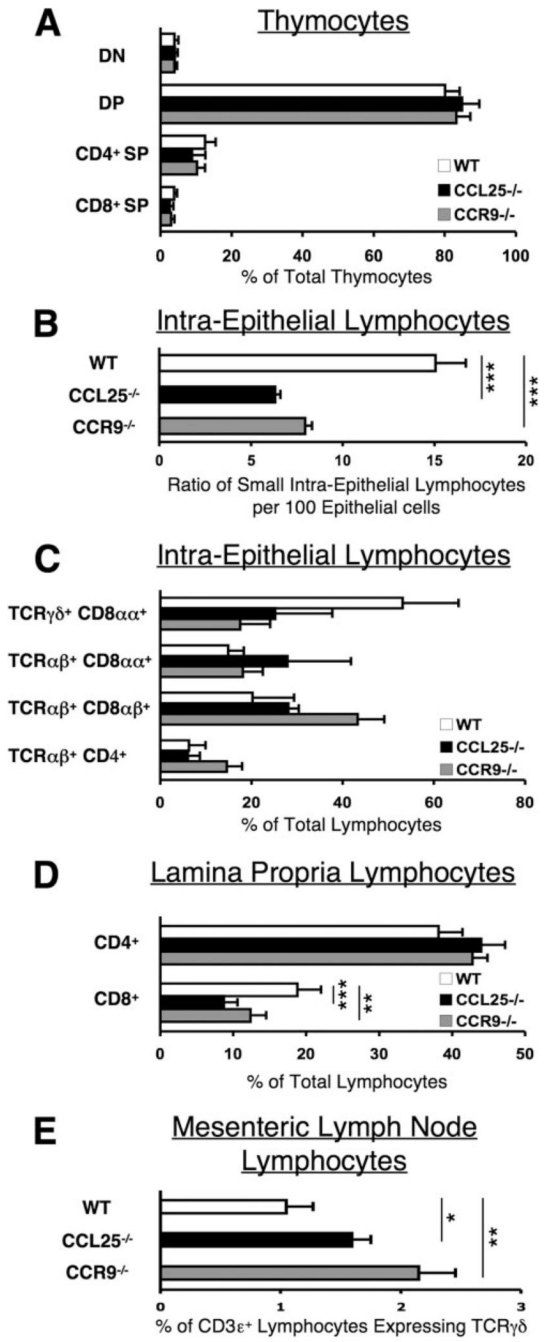

Figure 3.

Analysis of subset composition within thymus, small intestine compartments and MLN of WT and CCL25-deficient mice. *A*, The percentage of DN, DP, $CD4^+$ SP, and $CD8^+$ SP thymocytes are shown for thymocytes from WT, $CCL25^{-/-}$, and $CCR9^{-/-}$ mice, as indicated (gated by scatter and CD4 vs CD8 expression). Mean and SEM are shown for 10 experiments. No significant differences were detected among the three different genotypes. *B*, Ratio of small IEL per 100 EC was assessed on duodenal tissue sections from WT, $CCL25^{-/-}$, and $CCR9^{-/-}$ intestines, as indicated. Mean and SEM are shown for six experiments. Values of p for divergence from WT ratios were calculated by ANOVA with Bonferroni correction as indicated by asterisks (***, $p < 0.001$). *C*, The percentage of major IEL subsets are shown from

WT, CCL25$^{-/-}$, and CCR9$^{-/-}$ small intestine, as indicated. Mean and SEM are shown for 12 experiments. *D*, The percentage of LPL T cell subsets (as percent of total lymphocytes) is shown from WT, CCL25$^{-/-}$, and CCR9$^{-/-}$ small intestines, as indicated. LPL were stained with CD3ε, CD4, CD8, and B220 mAbs, and analyzed by flow cytometry. Data are presented as mean ± SEM for 12 experiments. Values of *p* for divergence from WT ratios were calculated by an ANOVA with Bonferroni correction as indicated by asterisks (***, $p < 0.001$; **, $p < 0.01$). *E*, The percentage of TCR$\gamma\delta^+$ T cell subset (as percent of total CD3ε^+ T lymphocytes) in MLN is depicted for WT, CCL25$^{-/-}$, and CCR9$^{-/-}$ mice. Mean and SEM are shown for six experiments. Values of *p* for divergence from WT ratios were calculated by an ANOVA with Bonferroni correction as indicated by asterisks (*, $p < 0.01$; **, $p < 0.001$).

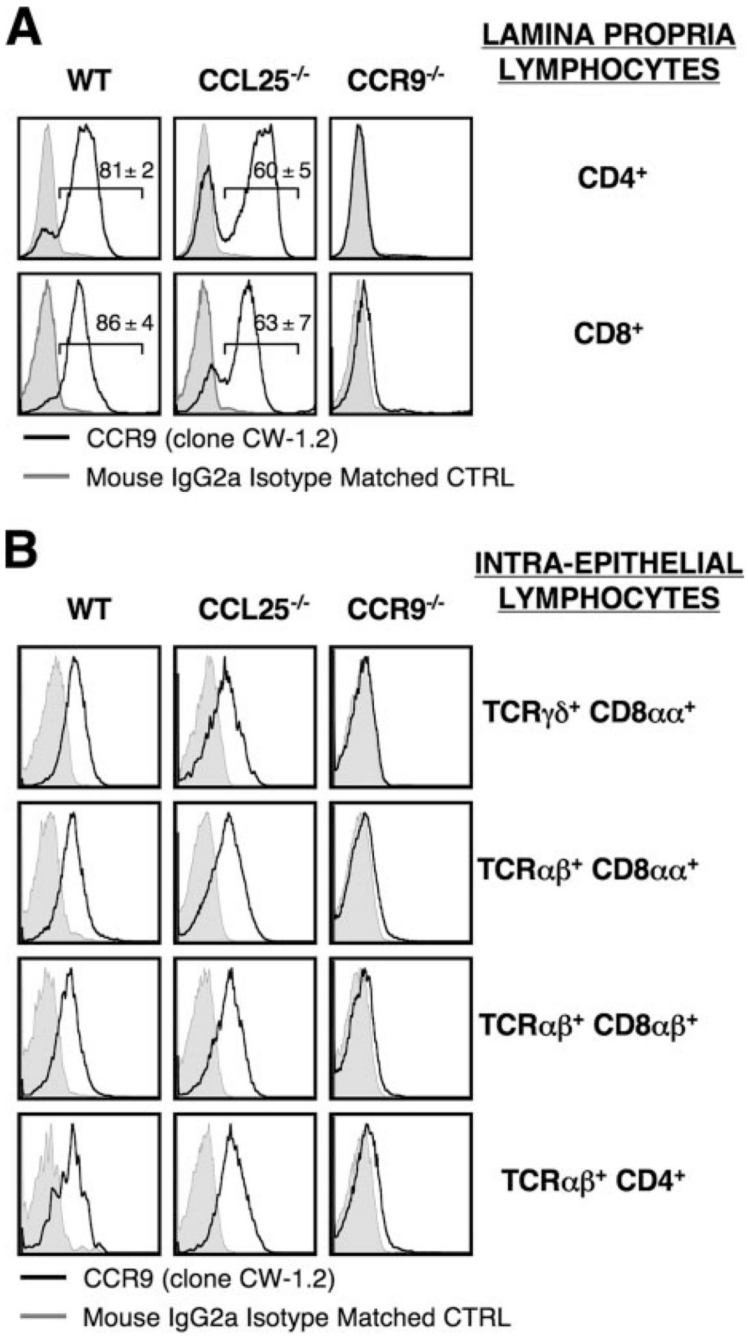

Figure 4.

CCR9 cell surface expression on LPL and IEL. *A*, Whole LPL from WT, CCL25-deficient, and CCR9-deficient mice were obtained by collagenase/DNase digestion of WT, CCL25-deficient, and CCR9-deficient small intestines after elimination of all IEL with EGTA. $CD4^+$ and $CD8^+$ LPL were stained with anti-CCR9 mAb (clone CW-1.2, in black) overlaid on mouse IgG2a-matched isotype control (in gray) and analyzed by flow cytometry. Data are from one representative experiment of six with similar results. *B*, Flow cytometry analysis of CCR9 cell surface expression (clone CW-1.2, in black) on major small intestinal IEL subsets from WT, CCL25-deficient, and CCR9-deficient mice (TCR$\gamma\delta^+$ CD8$\alpha\alpha^+$, TCR$\alpha\beta^+$ CD8$\alpha\alpha^+$,

TCR$\alpha\beta^+$ CD8$\alpha\beta^+$, and TCR$\alpha\beta^+$ CD4$^+$) overlaid on mouse IgG2a matched isotype control. Data are from a single representative experiment of six repeats.

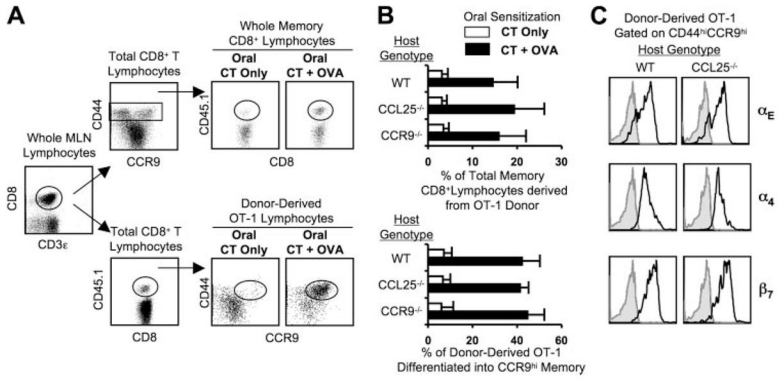

Figure 5.

Ag-specific CCR9^{high} memory MLN lymphocytes are generated in the absence of CCL25 chemokine expression. Splenocytes were isolated from CD45.1^{+} OT-1 TCR-Tg mice and adoptively transferred into CD45.2^{+} WT hosts. The hosts were then orally sensitized with OVA + cholera toxin (CT) or with CT alone. Four days after oral sensitization, MLN lymphocytes were harvested and analyzed by flow cytometry. *A*, Two different cytometry gating schemes are shown for analyzing OT-1 cells in adoptive hosts after oral immunization with OVA + CT or CT only. The gating scheme on *top* displays the percentage of total memory CD8 T cells within the host MLN that were derived from the OT-1 donor after oral immunization, and was used to calculate the data shown in part *B*, *upper panel*. The gating scheme on the *bottom* displays the percentage of donor OT-1 CD8 T cells that have differentiated into CD44^{high}/CCR9^{high} memory cells after oral immunization, and was used to calculate the data shown in part *B*, *lower panel. B*, Generation of CCR9^{high} memory-phenotype OT-1 cells in WT, CCL25$^{-/-}$, and CCR9$^{-/-}$ MLN using gating criteria described in *A*. Percentages of donor-derived OT-1 cells that differentiated into CCR9^{high} memory-phenotype (*lower panel*) and percentage of total memory CD8^{+} lymphocytes derived from OT-1 donor (*upper panel*) are shown. Data are presented as mean and SEM of eight experiments. No significant differences were detected among the three different genotypes in ANOVA with Bonferroni correction. *C*, Expression of α_E, α_4, and β_7 integrins by donor-derived OT-1 cells that differentiated into CCR9^{high} memory. CCR9^{high} differentiated donor-derived OT-1 memory lymphocytes in WT and CCL25-deficient hosts depicted in *A* and *B* (*lower panel*) were staining with anti-α_E (clone M290), anti-α_4 (clone 9C10), and anti-β_7 (clone FIB-504) mAbs (black lines) and overlaid on isotype-matched rIgG$_{2a}$ controls (gray filled curves). Data are from a single representative experiment of three repeats.

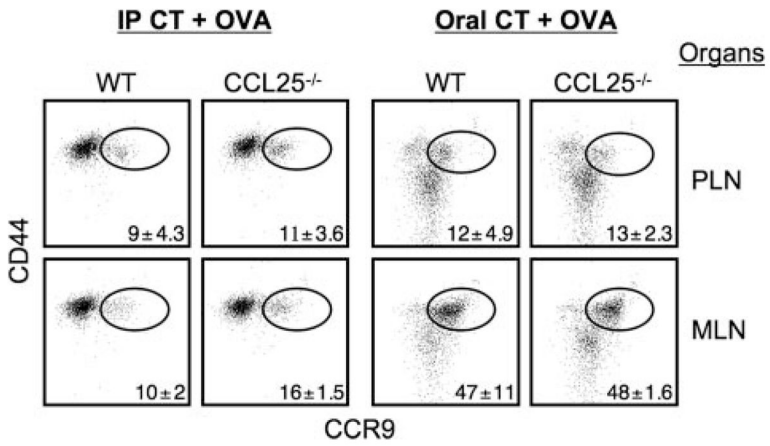

Figure 6.

Response to oral immunization, but not i.p. immunization, results in differentiation of intestinal memory-phenotype cells that are largely restricted to intestine and GALT. Naive CD45.1$^+$ OT-1 TCR-Tg lymphocytes were isolated and adoptively transferred into CD45.2$^+$ WT and CD45.2$^+$ CCL25-deficient recipient mice. The hosts were then treated either orally or i.p. with OVA + CT. Four days after sensitization, PLN and MLN lymphocytes were harvested and analyzed by flow cytometry as depicted in Fig. 5 (*A* and *B*, *lower panel*). The gating scheme displays the percentage of donor OT-1 CD8 T cells that have differentiated into CD44^{high}/CCR9^{high} memory cells after i.p. (*left*) and oral (*right*) immunization obtained in PLN (*upper panel*) and in MLN (*lower panel*) in WT and CCL25-deficient host mice. Dot plots are from a single representative experiment of four repeats.

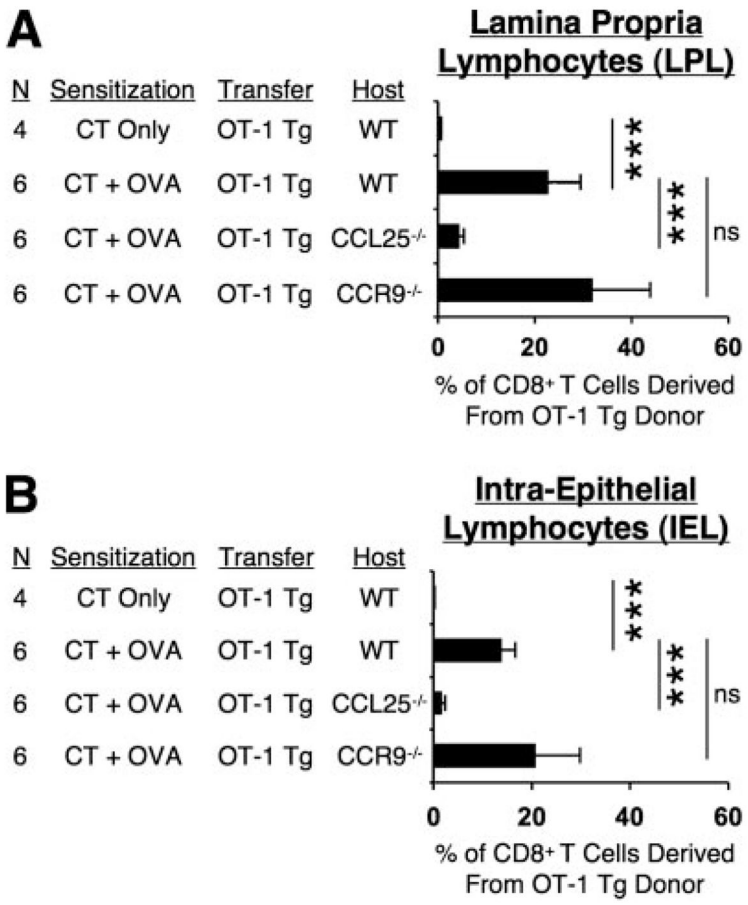

Figure 7.

Ag-specific lymphocyte homing to small intestine LP and epithelium is dramatically impaired in CCL25-deficient mice. *A*, Lamina propria $CD8^+$ T lymphocytes (LPL) and (*B*) intraepithelial $CD8^+$ lymphocytes (IEL) were harvested, stained, and analyzed by flow cytometry. The percentage of total $CD8^+$ T cells derived from the OT-1 donor at day 4 after oral gavage is shown. Data are presented as the mean and SEM of four or six mice as indicated by N. Values of *p* as calculated by ANOVA with Bonferroni correction as indicated by asterisks (***, $p < 0.05$; ns: not significant).

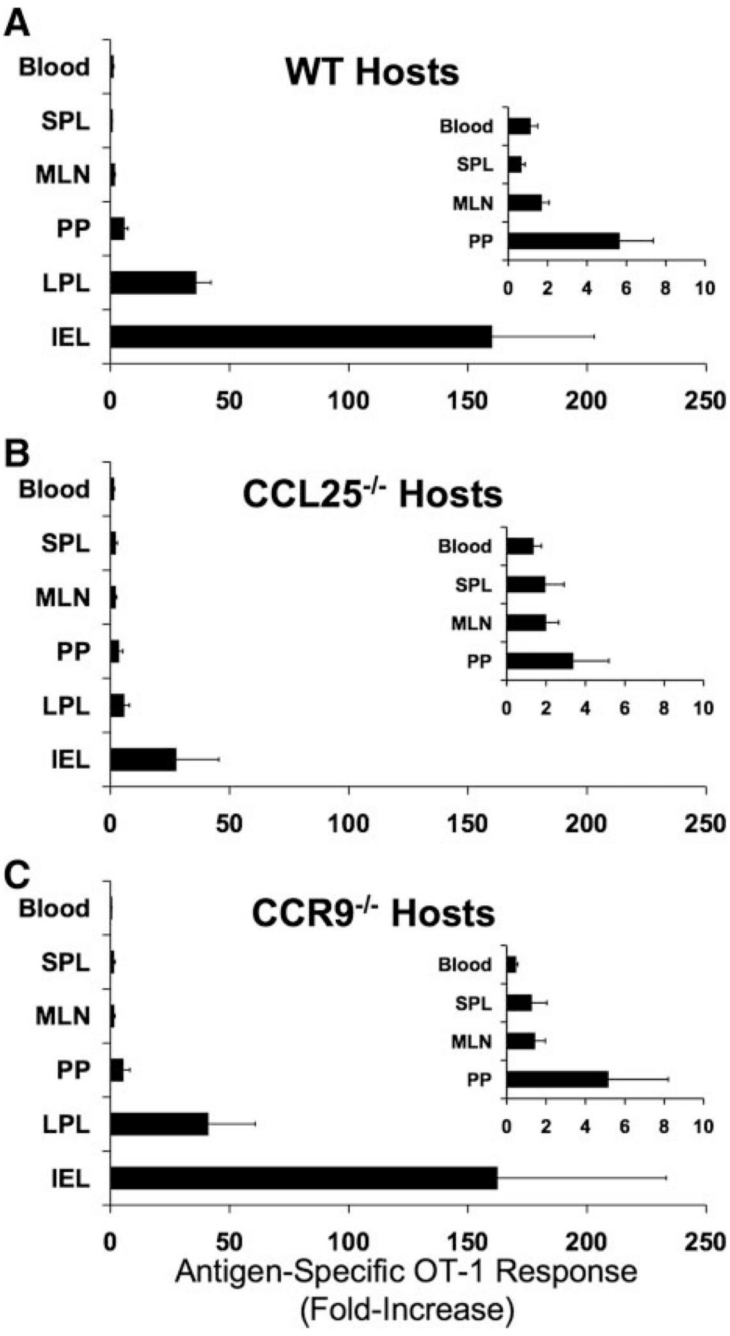

Figure 8.

Ag-specific enrichment of OT-1 lymphocytes after oral gavage is specific to intestine-associated tissues. Ag-specific fold-increase in OT-1 representation was calculated for the total $CD8^+$ T cell populations between pairs of mice treated with CT only or OVA + CT in various organs at day 4 after oral gavage. The ratios were calculated for blood, SPL, MLN, PP, LPL, and IEL. This was calculated for (*A*) WT hosts, (*B*) $CCL25^{-/-}$ hosts, and (*C*) $CCR9^{-/-}$ hosts. Mean and SEM are shown for four pairs of mice for each genotype. The differences between WT and $CCL25^{-/-}$ hosts were highly significant for LPL ($p < 0.05$) and IEL ($p < 0.001$) by ANOVA test with Bonferroni correction, but were not significant between WT and $CCR9^{-/-}$

hosts. *Insets* for each genotype (*A–C*) show the identical data for only lymphoid organs on a smaller scale.